doi:10.1016/j.jmb.2005.05.034 J. Mol. Biol. (2005) 350, 1083–1093

JMB

Available online at www.sciencedirect.com

SCIENCE DIRECT®

ELSEVIER

The Activation Mechanism of Hsp26 does not Require Dissociation of the Oligomer

Titus M. Franzmann, Martin Wühr, Klaus Richter, Stefan Walter and Johannes Buchner*

Department Chemie, Technische Universität München, 85747 Garching, Germany

*Corresponding author

Small heat shock proteins (sHsps) are molecular chaperones that specifically bind non-native proteins and prevent them from irreversible aggregation. A key trait of sHsps is their existence as dynamic oligomers. Hsp26 from *Saccharomyces cerevisiae* assembles into a 24mer, which becomes activated under heat shock conditions and forms large, stable substrate complexes. This activation coincides with the destabilization of the oligomer and the appearance of dimers. This and results from other groups led to the generally accepted notion that dissociation might be a requirement for the chaperone mechanism of sHsps.

To understand the chaperone mechanism of sHsps it is crucial to analyze the relationship between chaperone activity and stability of the oligomer. We generated an Hsp26 variant, in which a serine residue of the N-terminal domain was replaced by cysteine. This allowed us to covalently crosslink neighboring subunits by disulfide bonds. We show that under reducing conditions the structure and function of this variant are indistinguishable from that of the wild-type protein. However, when the cysteine residues are oxidized, the dissociation into dimers at higher temperatures is no longer observed, yet the chaperone activity remains unaffected. Furthermore, we show that the exchange of subunits between Hsp26 oligomers is significantly slower than substrate aggregation and even inhibited in the presence of disulfide bonds. This demonstrates that the rearrangements necessary for shifting Hsp26 from a low to a high affinity state for binding non-native proteins occur without dissolving the oligomer.

Keywords: small heat shock protein; molecular chaperone; alpha crystallin; aggregation; disulfide bond

Introduction

Small heat shock proteins (sHsps) belong to the functionally related class of molecular chaperones that specifically recognize non-native proteins.[1–3] As part of the cellular multi-chaperone network, sHsps possess a substantial binding capacity for protein folding intermediates, which allows them to prevent their irreversible aggregation.[4–8] sHsps are characterized by several structural and functional features. The most significant is the presence of the highly conserved α-crystallin domain in the C-terminal part of the proteins.[9,10] In αA and αB-crystallin, the two major eye lens proteins in vertebrates, these domains are composed of about 80 residues with 60% sequence identity.[11,12] Besides this, sHsps share monomeric masses between 12 kDa and 43 kDa. These monomers associate into oligomeric structures with mostly 12 or 24 subunits. Even larger complexes with up to 50 subunits were observed for α-crystallin.[13,14] The large variability in the length of the N-terminal regions appears to be responsible for the significant variations of the sizes of the oligomers.[12] So far, two

Abbreviations used: sHsps, small heat shock proteins; AIAS, 4-acetamido-4′-((iodoacetyl)amino)stilbene-2,2′-disulfonic acid; CD, circular dichroism; CS, citrate synthase; DTNB, 5,5′-dithiobis(2-nitrobenzoic acid); $DTT_{(red)}$, reduced form of dithiothreitol; $DTT_{(ox)}$, oxidized form of dithiothreitol; FITC, fluorescein isothiocyanate; GdmCl, guanidin hydrochloride; GSSG, oxidized glutathione; IAA, iodoacetamide; LYI, lucifer yellow iodoacetamide; SEC, size exclusion chromatography; TAMRA, tetramethylrodhamine; TEM, transmission electron microscopy.

E-mail address of the corresponding author: johannes.buchner@ch.tum.de

X-ray structures of sHsps have been resolved. Hsp16.5 from *Methanocaldococcus jannaschii* assembles into a 24mer and forms a hollow sphere with octahedral symmetry.[15] Hsp16.9 from wheat forms a 12mer arranged into two hexameric rings.[16] Both structures revealed the α-crystallin domain as the dimeric building block. In addition to the α-crystallin domain, sHsps comprise a flexible, disordered N-terminal region and a C-terminal extension. From structural investigations carried out for various sHsps, including Hsp16.5, α-crystallin and Hsp16.2 from *Caenorhabditis elegans*, it was proposed that the N-terminal regions are sequestered inside the oligomers.[15,17,18] Recently it was shown that the N-terminal regions are required for substrate interactions[19] and that they play a role in stabilizing the oligomeric state.[20,21] The C-terminal extensions appear to be moderately conserved throughout the sHsps family. In Hsp16.5, these were found to mediate the self-association into the oligomeric complex *via* inter-subunit interactions.[15] This was confirmed for various sHsps in which the C-terminal extensions were either removed or mutated.[21–24] Mostly these variants fail to associate into their native quaternary structure. The N-terminal region and the C-terminal extension seem to have partially overlapping functions with respect to the association of the oligomer. Furthermore, both regions are required for efficient chaperone activity[20,24] and recent investigations suggest that oligomerization of sHsps is a prerequisite for their chaperone mechanism.[17,21,25–28] sHsps are dynamic structures, which permanently exchange subunits between oligomers.[29–33] Although this dynamic behavior seems to be a common feature, no functional importance could be assigned to it so far and it was speculated that the exchange of subunits is linked to the chaperone mechanism.

Hsp26 is one of the two cytosolic sHsps from *Saccharomyces cerevisiae*.[34] Under physiological conditions, it exists as a hollow sphere of 24 subunits assembled from 12 dimers.[35–37] We have shown previously that Hsp26 efficiently suppresses heat-induced aggregation of substrates *in vivo* and *in vitro* and associates into defined, stable complexes with model substrates including citrate synthase (CS) and insulin, indicating promiscuous binding properties.[6,7,38] The first 30 amino acid residues of the N-terminal domain of Hsp26 are required for substrate interaction and stabilize the oligomeric state.[20] Residues 30–95 play a role in the association of the native oligomer.[19] An important functional characteristic is that Hsp26 requires elevated temperatures for activation, as it fails to efficiently suppress the reduction-induced aggregation of insulin at room temperature.[38] Coinciding with the temperature-dependent activation, the Hsp26 oligomer was shown to become destabilized and dissociate into dimers.

To gain further insight into the chaperone mechanism of sHsps, we generated a point mutant of Hsp26, in which the residue serine 4 of the N-terminal domain ($Hsp26_{S4C}$) was replaced by cysteine. The introduction of this reactive residue allowed covalent cross-linking of neighboring subunits by oxidation. Analysis of the structure and function under reducing conditions showed that $Hsp26_{S4C}$ behaved indistinguishably from the Hsp26 wild-type protein. Interestingly, when the cysteine residues were oxidized, the Hsp26 oligomer was stabilized and subunit exchange and dissociation into dimers was completely inhibited, yet the chaperone activity remained unaffected. These results show that the rearrangements necessary for activation of Hsp26 can occur without dissolving the oligomer and indicate that the Hsp26 oligomer can interact with substrate proteins.

Results

Structural analysis of reduced and oxidized $Hsp26_{S4C}$

sHsps consist of a predominantly β-structured α-crystallin domain,[9,10] an unstructured N-terminal region and a moderately conserved C-terminal extension. Since truncations in the N-terminal regions affect the stability of the oligomeric structure, it was tempting to speculate that the N-terminal regions are involved in inter-subunit interactions. The introduction of artificial disulfide bridges in proteins had been used successfully to analyze the importance of conformational rearrangements in chaperone mechanisms.[39] Thus, we generated a variant of Hsp26 in which the residue S4 of the N-terminal region was replaced by cysteine ($Hsp26_{S4C}$). It should be noted that the Hsp26 wild-type protein does not contain cysteine residues.

First, we analyzed the cysteine variant with respect to its ability of disulfide bond formation. Quantification of the reduced samples with the DTNB reaction revealed one free cysteine per subunit, indicating that all cysteine residues were accessible and reduced (data not shown). In agreement with this, we determined a specific labelling efficiency of one fluorescence probe per subunit by UV spectroscopy (data not shown). No free thiol groups were present after IAA treatment, showing that all cysteine residues were blocked covalently (data not shown). Testing the oxidized form revealed 0.3 free cysteine residue in $Hsp26_{S4C}$ (data not shown). In agreement, we found that ~2/3 of the subunits were cross-linked by disulfide bond formation with SDS-PAGE under non-reducing conditions (Figure 1). The cross-linking efficiency was not increased using other oxidative agents such as oxidized glutathione or air.

To test whether the mutation affected the structural integrity of the protein, we analyzed the secondary structure by circular dichroism (CD) spectroscopy. Hsp26 exhibits a minimum at ~214 nm with intensities of $-8500\ \mathrm{deg \cdot cm^2 \cdot dmol^{-1}}$ (Figure 2(a)). Deconvolution of the data

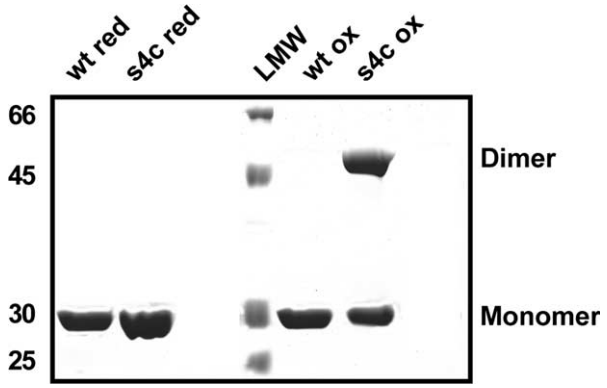

Figure 1. Non-reducing SDS-PAGE of Hsp26 and $Hsp26_{S4C}$. Samples were prepared as described in Materials and Methods with reducing or oxidizing DTT, respectively.

revealed 17% α-helical and 45% β-sheet content.[19] CD spectra of reduced and oxidized $Hsp26_{S4C}$ were indistinguishable from that of the wild-type protein (Figure 2(b)), indicating that the cysteine variant is natively folded under both reducing and oxidizing conditions.

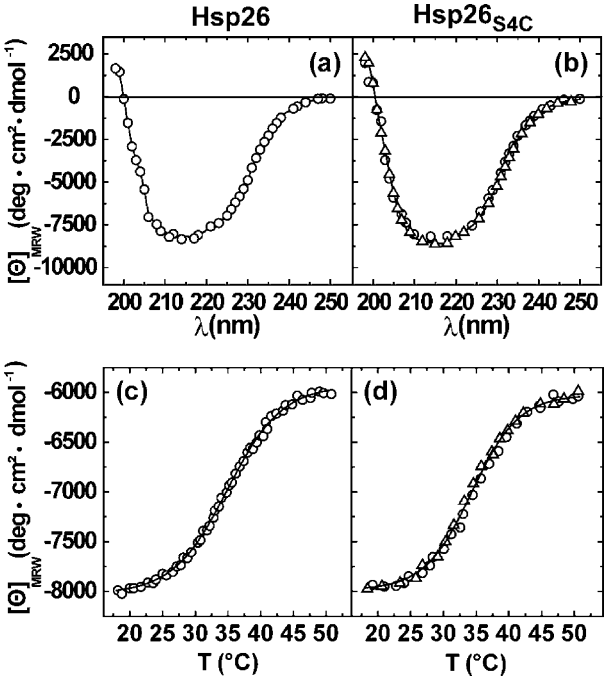

Figure 2. Far UV CD spectra and thermal transitions of Hsp26 and $Hsp26_{S4C}$. Spectra were recorded at 20 °C in 10 mM potassium phosphate (pH 7.5). (a) Far UV CD spectrum of 0.1 mg/ml Hsp26 (○). (b) Far UV CD spectra of 0.1 mg/ml of reduced (○) and oxidized (△) $Hsp26_{S4C}$. Temperature-induced changes in the far UV signal of the proteins were monitored at a constant wavelength of 220 nm. Transitions of 0.1 mg/ml were recorded in 10 mM potassium phosphate (pH 7.5) with a heating rate of 10 deg. C/hour. (c) Thermal unfolding of Hsp26 (○). (d) Thermal unfolding of reduced (○) and oxidized (△) $Hsp26_{S4C}$.

Hsp26 exhibits two thermal transition midpoints;[19] the first at ~36 °C (Figure 2(c)) and a second at ~74 °C (not shown). The first transition represents defined structure changes while the second transition leads to global unfolding. Here we analyzed the first transition, which occurs at physiologically relevant conditions. It should be noted that Hsp26 exhibits chaperone activity at these temperatures. These temperature-induced structural changes in Hsp26 thus do not refer to thermal-induced denaturation, but coincide with the activation of the chaperone. The midpoint of the thermal transition of the wild-type protein was at 36 °C and the structural transition was reversible when the sample was heated to 55 °C only. The ΔG value calculated for this transition was 7.3 (±1.1) kJ/mol. The oxidized and reduced cysteine variant exhibits reversible transitions with identical transition midpoints and ΔG values (Figure 2(d)), demonstrating that the transitions are unaffected by the redox state of the cysteine residues.

Further, we analyzed the tertiary structure of Hsp26 and the reduced and oxidized cysteine variants by near UV spectroscopy. Analysis of Hsp26 at 25 °C revealed maxima at 294 nm and 285 nm due to the absorbance of tryptophan residues, a maximum at 278 nm due to tyrosine absorbance and a broad minimum around 265 nm due to phenylalanine absorbance[40] (Figure 3(a)). Similar spectra were obtained for the reduced and oxidized cysteine variant at 25 °C, indicating that the tertiary structure is highly similar under reducing and oxidizing conditions (Figure 3(b) and (c)). Analysis of Hsp26 at 45 °C revealed intensity changes at 294 nm, 285 nm and 265 nm (Figure 3(a)). The tyrosine absorbance signal at 278 nm remained unchanged. Analysis of the reduced cysteine variant also revealed changes at 294 nm, 285 nm and 268 nm, demonstrating that the reduced form undergoes identical temperature-induced changes (Figure 3(b)). Interestingly, analysis of the oxidized variant at elevated temperatures revealed comparable changes in the tertiary structure (Figure 3(c)). However, additionally the signal intensities at 278 nm were altered, due to the presence of disulfide bonds. This demonstrates that cross-linking subunits by oxidation did not prevent Hsp26 tertiary structure changes. It is notable that temperature-induced changes of the tertiary structure in Hsp26 mainly affect the absorbance signals at 268 nm corresponding to rearrangements of phenylalanine residues. Interestingly, nine of a total of 11 phenylalanine residues are located within the N-terminal region of Hsp26.

Hsp26 is a temperature-regulated sHsp.[38] The activation coincides with the destabilization of the oligomer and the appearance of dimers. To determine whether the redox state of the cysteine variant affected the dynamics and stability of the oligomer, we performed gel filtration experiments under oxidizing and reducing conditions. At room temperature (25 °C), Hsp26 eluted as a 24mer (Figure 4(a), straight line). Identical profiles were

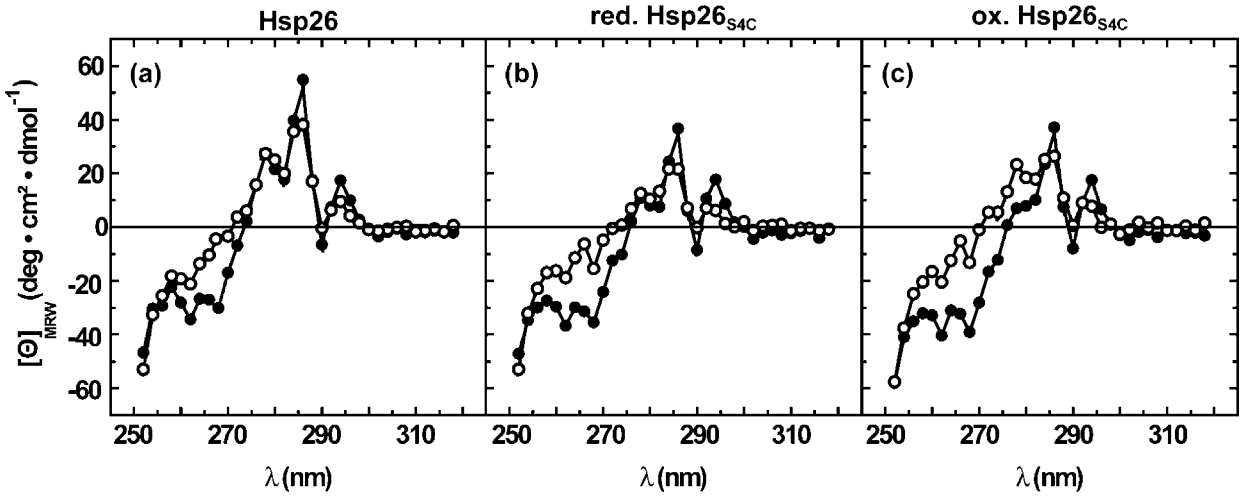

Figure 3. Temperature-induced tertiary structure changes of Hsp26 and Hsp26$_{S4C}$. Near UV CD spectra of 1 mg/ml Hsp26 and Hsp26$_{S4C}$ were recorded at 25 ° and 45 °C, respectively, in 10 mM potassium phosphate (pH 7.5). (a) Hsp26 at 25 °C (●) and 45 °C (○); (b) reduced Hsp26$_{S4C}$ at 25 °C (●) and 45 °C (○); (c) oxidized Hsp26$_{S4C}$ at 25 °C (●) and 45 °C (○).

obtained for the cysteine variant of Hsp26 under reducing (Figure 4(b), straight line) and oxidizing conditions (data not shown). In agreement with previous results,[19,38] Hsp26 eluted as a dimer at elevated temperature (Figure 4(a), dotted line). Prolonged incubation of Hsp26 at elevated temperatures and subsequent analysis by analytical SEC at 44 °C over a period of six hours did not shift the elution profiles towards larger species, showing that the dimer is a stable exchangeable unit (data not shown). Analysis of Hsp26$_{S4C}$ at 44 °C and reducing conditions (Figure 4(b), dotted lines) revealed that the protein was also destabilized and eluted as dimers. However, under oxidizing conditions, the oligomeric complex was significantly stabilized and Hsp26$_{S4C}$ eluted as an oligomer of 24 subunits, with elution times equal to that at 25 °C (Figure 4(b), broken lines). This shows that the dissociation of the oligomer into dimers is inhibited in the presence of disulfide bonds. The question remained, whether the oxidized variant exhibits dynamic subunit exchange. To analyze this, we labelled Hsp26 and the reduced and oxidized proteins with fluorescent dyes and monitored the exchange of subunits by fluorescence resonance energy transfer (FRET). At 25 °C, we measured a subunit exchange rate of $k_{transfer} = 4.9 \times 10^{-4}\,s^{-1}$ with a half-life of $t_{1/2} \sim 1400$ s for Hsp26 (Figure 4(a) and (c)) and reduced Hsp26$_{S4C}$ (Figure 5(d), squares). At 40 °C, the rate of subunit exchange was increased by one order of magnitude, giving a rate $k_{transfer} = 4.4 \times 10^{-3}\,s^{-1}$ and a half-life of ~158 seconds for both, Hsp26 (Figure 5(b) and (c)) and reduced Hsp26$_{S4C}$ (data not shown). The subsequent addition of a 40-fold excess of unlabelled Hsp26 to the mixed oligomers led to the complete reversion of the FRET signals, showing that subunit exchange of Hsp26 is a dynamic and reversible process (Figure 5(d), triangles). However, subunit exchange was not detected for oxidized Hsp26$_{S4C}$. This was not due to the low labelling efficiency of the oxidized species, as unlabelled, oxidized Hsp26$_{S4C}$ was unable to disrupt the FRET signal of mixed Hsp26 oligomers (Figure 5(d), circles). This demonstrates that in the presence of disulfide bonds the dynamics and stability of the oligomeric complex are strongly affected and that subunit exchange and dissociation of Hsp26 are completely inhibited.

Chaperone activity of Hsp26$_{S4C}$

The oxidized cysteine variant allowed us to investigate whether the destabilization of the Hsp26 oligomer at higher temperatures and the subsequent dissociation into dimers are essential for the chaperone function of Hsp26. As shown previously, thermally induced aggregation of CS was efficiently prevented in the presence of a twofold excess of Hsp26 (Figure 6(a)).[38] Analysis of reduced Hsp26$_{S4C}$ revealed that the protein exhibits chaperone activity indistinguishable from that of the wild-type protein (Figure 6(b)). Surprisingly, the chaperone activity of oxidized Hsp26$_{S4C}$ was identical to that of the reduced protein (Figure 6(c)). Previously we reported that incubation of Hsp26 with CS at elevated temperatures leads to the formation of high molecular mass substrate complexes with diameters of ~50 nm.[6,38] Analysis by analytical SEC showed that the substrate complexes between CS and Hsp26 were formed efficiently (Figure 6(d)) and that the substrate complexes of CS and the reduced or oxidized form of the cysteine variant did not reveal any significant differences (Figure 6(e) and (f)). This was confirmed by electron microscopy of the substrate complexes (Figure 6(g)–(i)). In all cases, round-shaped substrate complexes with diameters of 40–60 nm were observed. Taken together, these

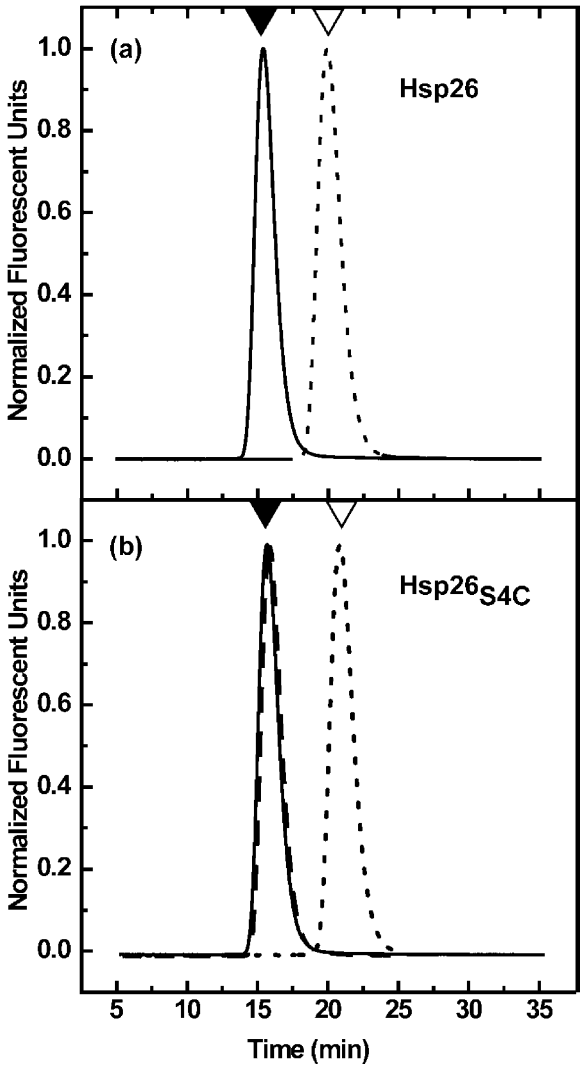

Figure 4. Temperature-dependent quaternary structure analysis of Hsp26 and reduced and oxidized $Hsp26_{S4C}$. SEC was carried out using a TosoHaas TSK G4000PW equilibrated at either 25 °C or 44 °C in 40 mM Hepes (pH 7.5), 150 mM KCl, 5 mM EDTA. (▼) Indicates the elution peak of the Hsp26 oligomer, (▽) the elution peak of the Hsp26 dimer. (a) Hsp26 at 25 °C (continuous line) and at 44 °C (dotted line); (b) $Hsp26_{S4C}$ at 25 °C (continuous line), at 44 °C under reducing (dotted line) and oxidizing (broken line) conditions.

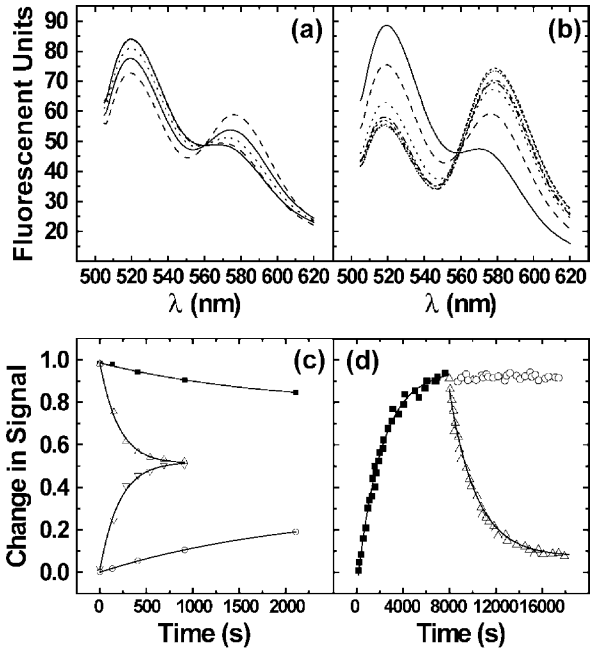

Figure 5. Subunit exchange of Hsp26 and $Hsp26_{S4C}$. Subunit exchange between Hsp26 oligomers was measured by fluorescence resonance energy transfer in 40 mM Hepes (pH 7.5). Time-dependent changes in emission spectra of 5 μM FITC and 5 μM TAMRA labelled Hsp26 at (a) 25 °C and (b) 40 °C. (c) Time-dependent changes in donor (■) and acceptor emission intensities (○) at 25 °C and, changes in donor (△) and acceptor emission (▽) intensities at 40 °C. (d) Subunit exchange of AIAS and LYI labelled $Hsp26_{S4C}$. (■) Subunit exchange of 1 μM $Hsp26_{S4C}$. (△) FRET displacement by the subsequent addition of a 40-fold excess of unlabeled Hsp26 and (○) of oxidized, unlabelled $Hsp26_{S4C}$.

results demonstrate that dissociation of Hsp26 is not required for chaperone activity.

For Hsp26, elevated temperatures are essential to display chaperone activity. The question remained, whether the mutant also requires elevated temperatures for its activation. Testing the proteins at room temperature with chemically unfolded CS, we found that neither the wild-type protein, nor the reduced or oxidized Hsp26 variant exhibit chaperone activity (Figure 7(a)–(c), circles). This shows that the oxidized variant is not trapped within a permanently active state. Next, we tested whether the heat-activated state persists after shifting Hsp26 back from elevated temperatures to room temperature. Interestingly, after incubation of Hsp26 at elevated temperatures, reduced and oxidized $Hsp26_{S4C}$ suppressed substrate aggregation at room temperature, demonstrating that Hsp26, the reduced and oxidized variant require heat-treatment to gain chaperone activity. In agreement with our results for heat-induced aggregation of CS, aggregation of chemically denatured CS was predominantly suppressed with a twofold excess of chaperone (Figure 7(a)–(c), triangles). When heat-treated Hsp26 was incubated for 45 minutes at room temperature it was completely inactive again, demonstrating that this activation is a reversible process (data not shown). Comparison of the half-life of subunit exchange at 25 °C ($t_{1/2} \sim 1400$ s) to that of the aggregation of unfolded CS at 25 °C ($t_{1/2} \sim 17$ s) illustrates that subunit exchange between Hsp26 oligomers is significantly slower than substrate aggregation (Figure 7(d)).

Quaternary structure analysis of Hsp26 under equilibrium conditions

Our results on the cysteine variant required

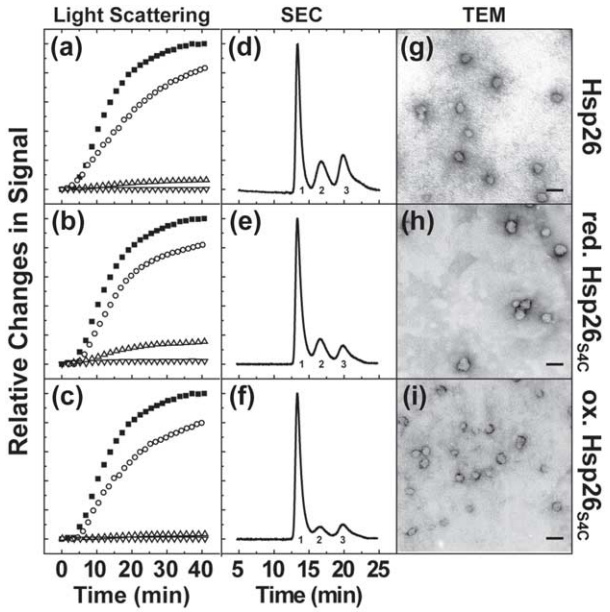

Figure 6. Chaperone activity of reduced and oxidized $Hsp26_{S4C}$. Chaperone activity and complex formation was determined by light scattering ((a)–(c)), SEC ((d)–(f)) and TEM ((g)–(i)), respectively. Heat-induced aggregation of 1 μM CS at 44 °C in 40 mM Hepes (pH 7.5) in the presence of 0 μM (■), 1 μM (○) and 2 μM (△) and 4 μM (▽) molecular chaperone. (a) Hsp26; (b) reduced $Hsp26_{S4C}$; (c) oxidized $Hsp26_{S4C}$. SEC analysis of substrate complex formation with 2 μM chaperone and 1 μM CS. Numbers in the graphs refer to the substrate complex (1), free Hsp26 (2) and free CS (3), respectively. (d) Hsp26; (e) reduced $Hsp26_{S4C}$; (f) oxidized $Hsp26_{S4C}$. TEM analysis of CS substrate complexes with (g) Hsp26, (h) reduced $Hsp26_{S4C}$; (i) oxidized $Hsp26_{S4C}$. Bars represent 100 nm.

further analysis of Hsp26 with respect to the stability of the oligomeric complex. With subunit exchange experiments we had analyzed the dynamic behavior of Hsp26 at various temperatures. However, these results do not fully describe the oligomerization equilibrium of Hsp26, though they indicate that the Hsp26 oligomer is also present at elevated temperatures, since FRET was detectable at 40 °C. We therefore wanted to know whether the quaternary structure of Hsp26 is shifted in a temperature-dependent way from its oligomeric state towards the dimer under equilibrium conditions. In ultracentrifugation sedimentation experiments with Hsp26 at 25 °C, we obtained a single apparent sedimentation coefficient of 22 S, demonstrating that Hsp26 sediments as an oligomeric species (Figure 8(a) and (d)). Sedimentation experiments at 30 °C, 35 °C (data not shown) and 40 °C also revealed sedimentation coefficients of ~22 S (Figure 8(b) and (d)). A fivefold reduction in the concentration of Hsp26 did not shift the oligomerization equilibrium towards smaller species (data not shown). For Hsp26ΔN, a variant of Hsp26 lacking the N-terminal region, which assembles into dimers only,[19] we determined a sedimentation coefficient of 1.9 S at 25 °C (data not shown) and at 40 °C (Figure 8(c) and (d)), respectively. Taken together these results show that the rate for the exchange of subunits between oligomers increases temperature-dependently, nevertheless the oligomerization equilibrium remains unaffected. Thus Hsp26 becomes destabilized at elevated temperatures but this does not necessarily lead to the complete dissociation into dimers.

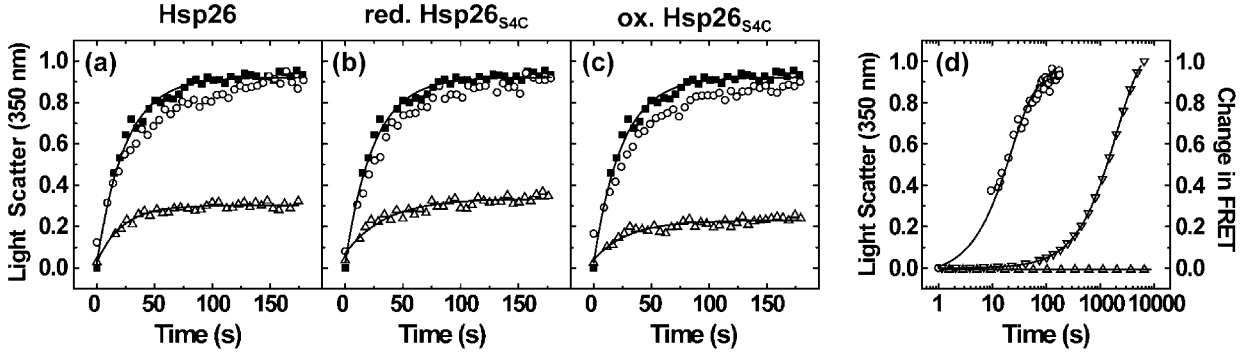

Figure 7. Chaperone activity of Hsp26 with chemically unfolded CS. CS was prepared as described in Materials and Methods. CS aggregation was induced by diluting the substrate 100-fold into 40 mM Hepes (pH 7.5), 2 mM GSH or 1 mM GSSG, respectively, at 25 °C. (a) Aggregation of 150 nM CS in the absence of chaperone (■), in the presence of 300 nM Hsp26 (○) and in the presence of heat-treated Hsp26 (△). (b) Aggregation of 150 nM CS in the absence of chaperone (■), in the presence of 300 nM reduced $Hsp26_{S4C}$ (○) and in the presence of reduced and heat-treated $Hsp26_{S4C}$ (△). (c) Aggregation of 150 nM CS in the absence of chaperone (■), in the presence of 300 nM oxidized $Hsp26_{S4C}$ (○) and in the presence of oxidized and heat-treated $Hsp26_{S4C}$ (△). Aggregation of chemically unfolded CS in the absence of sHsps was normalized to 1. ((d) Comparison between the velocities of the aggregation of chemically denatured CS (○) and the subunit exchange of reduced (▽) and oxidized $Hsp26_{S4C}$ (△) at 25 °C.

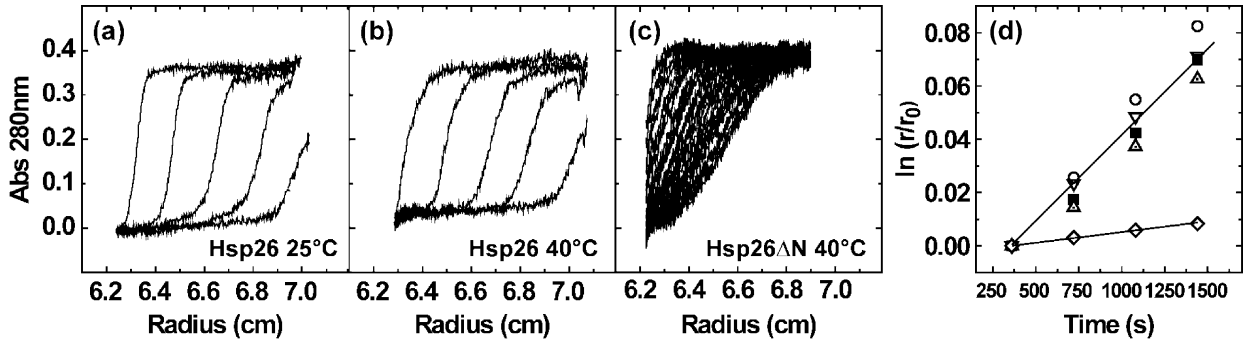

Figure 8. Analytical sedimentation ultracentrifugation analysis of Hsp26 and Hsp26ΔN. Analytical sedimentation ultracentrifugation was carried at various temperatures of Hsp26 and Hsp26ΔN. (a) Sedimentation profile of 0.3 mg/ml Hsp26 at 25 °C. (b) Sedimentation profile of 0.3 mg/ml Hsp26 at 40 °C. (c) Sedimentation profile of 0.5 mg/ml Hsp26ΔN. (d) Evaluation of sedimentation coefficients for Hsp26 protein at 25 °C (■), 30 °C (○), 35 °C (△) 40 °C (▽) and Hsp26ΔN at 40 °C (◇).

Discussion

sHsps form oligomeric structures, which bind non-native proteins in a cooperative and efficient manner.[3] It appears that this class of molecular chaperones can be divided into constitutively active and temperature-controlled sHsps. Hsp26 is a prototypic temperature-regulated sHsp, as it requires elevated temperatures to display chaperone activity. Previously, we reported that the complex of 24 subunits becomes destabilized upon heat-activation, resulting in the appearance of dimers in analytical gel filtration experiments.[38] At the same time, electron microscopy revealed that Hsp26 substrate-complexes were oligomeric structures. Both observations led to the notion that the heat-activation requires oligomer dissociation into dimers, which re-associate with substrate proteins to form large complexes.[6,38] Such a cooperative dissociation has not been observed for all sHsps, yet all of the so far investigated sHsps were reported to be dynamic oligomers exchanging subunits.[29–31,41] It is generally accepted that sHsps continuously dissociate into smaller units and re-associate. These observations led to the notion, that dissociation is a requirement for the chaperone activity of sHsps.[31,41] This raised the question whether the formation of dimers is an essential part in the chaperone mechanism of sHsps. We addressed this question by investigating an Hsp26 mutant that did not dissociate into dimers at elevated temperatures.

Previous structure analysis of sHsps suggested that the N-terminal regions are sequestered inside the oligomers.[15,42,43] Using the N-terminal cysteine variant, $Hsp26_{S4C}$, we were able to cross-link ~65% of the subunits. The cross-linking ratio suggests that the N termini form trimers. Under oxidizing conditions, two of three subunits form a disulfide bond, while the third remains reduced. This stoichiometry suggests an octahedral symmetry with eight trimerization sites of the N-terminal regions. Given that two Hsp26 subunits associate into antiparallel dimers, mediated by the α-crystallin domain,[15,43] the trimerization links six Hsp26 monomers. Such a hexameric arrangement of three dimers has been observed in the crystal structure of Hsp16.5.[15]

Our structural investigations revealed that reduced and oxidized $Hsp26_{S4C}$ adopts secondary and quaternary structures indistinguishable from that of the wild-type protein. However, under oxidizing conditions and in the presence of disulfide bonds the cysteine variant maintained its oligomeric state at elevated temperatures and did not dissociate into dimers. Further, oxidized $Hsp26_{S4C}$ did not exchange subunits, indicating a complete loss of the dynamics. According to our data, the oxidized cysteine variant exhibits chaperone activity identical to that measured for the wild-type protein. This implies that the rate of subunit exchange cannot be a major determinant for chaperone activity of sHsps. This conclusion is further supported by the observation that subunit exchange in Hsp26 at 25 °C occurs with a similar rate ($k_{transfer} = 4.9 \times 10^{-4}\ s^{-1}$ at 25 °C) compared to that of αA-crystallin ($k_{transfer} = 6.36 \times 10^{-4}\ s^{-1}$ at 37 °C).[41] Yet, while αA-crystallin, similar to Hsp25 or Hsp42,[6,7,29] displays chaperone activity at room temperature, Hsp26 does not. The half-life of $t_{1/2} >$ 1000 s, illustrates that the rate of the subunit exchange is significantly slower than the aggregation of chemically unfolded CS ($t_{1/2} = 17$ s). At elevated temperatures the dynamics increase as determined by subunit exchange experiments. Due to the principle of separation by SEC and the increased dynamics at elevated temperatures, the Hsp26 dimer is separated from the 24mer, disturbing the oligomerization equilibrium between the Hsp26 oligomer and association intermediates. This leads to the cooperative dissociation into stabile dimers. However, under equilibrium conditions the Hsp26 oligomer is the most abundant species, also at elevated temperatures.

As a consequence, the activation of Hsp26 at elevated temperatures does not require dissociation into dimers nor increased dynamics of subunit exchange. Rather the essential steps are temperature-induced, structural rearrangements within the

oligomer. These rearrangements can occur without the necessity of oligomer dissociation. A correlation between changes in structure and chaperone activity has also been observed for α-crystallin.[44,45] Using the two Hsp26 variants Hsp26ΔN30, lacking residues 1–30, and Hsp26ΔN, lacking the residues 1–95, we had previously shown that the N-terminal region of Hsp26 is bi-functional;[19,20] Residues 1–30 are essential for substrate interaction, and amino acid residues 30–95 are required for the correct assembly of the oligomer. While Hsp26ΔN30 exhibits a thermal transition similar to that of the wild-type protein,[20] this is no longer observed in Hsp26ΔN,[19] indicating that the transition may reflect rearrangements of residues 30–95. This region of the protein might represent a temperature-regulated relay, switching the oligomer between a low and high affinity state. This is in agreement with our result that temperature-activation coincides with tertiary structure changes to phenylalanine residues. Since nine of the 11 phenylalanine residues of Hsp26 are located within the N-terminal region, this can be seen as further evidence that the N-terminal region changes its structure at elevated temperatures.

In summary, we propose two alternative conformations for the Hsp26 oligomer with differing affinities for unfolded proteins of 24 subunits (Figure 9). At physiological temperatures, Hsp26 is in an inactive, low affinity state, which is unable to bind unfolded proteins. Presumably, the substrate binding sites are largely buried inside the oligomer. It is tempting to speculate that the N-terminal regions associate into trimers and stabilize the inactive state by inter-molecular "self-recognition". Upon temperature increase, the Hsp26 oligomer undergoes structural rearrangements, involving the N-terminal domain, which converts it into an active chaperone. In this high affinity conformation, the substrate binding sites become exposed and the Hsp26 oligomer is able to bind non-native proteins. This active state persists for some time after shifting to lower temperatures, until the inactive state is restored.

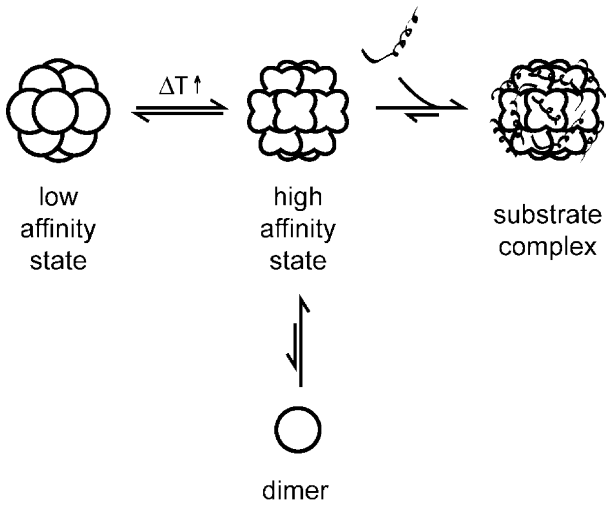

Figure 9. Model for the chaperone mechanism of a temperature-controlled sHsp. Hsp26 reversibly assembles from 12 dimers into the complex of 24 subunits. In the low affinity state Hsp26 does not interact with unfolded proteins. Elevated temperatures lead to conformational changes within the oligomer, thus switching the molecule from the low to the high affinity state. The Hsp26 oligomer becomes activated and associates with non-native proteins into the substrate complex.

Materials and Methods

Cloning and purification of Hsp26 and $Hsp26_{S4C}$

Structural genes of Hsp26 and the Hsp26 cysteine variants were amplified from genomic yeast DNA using PWO polymerase (Roche, Germany) with the following primers (Forward Hsp26: GAT CCC ATG GGG ATG TCA TTT AAC AGT C, Reverse Hsp26: GAT CGC GGC CGC TTA GTT ACC GTA CGA TTC TTG AGA AG, Forward $Hsp26_{S4C}$: GAT CCC ATG GGG TCA TTT AAC TGT CCA TTT TTT GAT TTC). The DNA fragments were ligated into pET28b+ (Novagene) and expressed in *Escherichia coli* BL21 (DE3) (Stratagene) at 30 °C for four hours. Expression was induced with 1 mM IPTG. The proteins were purified to homogeneity using a Q-Sepharose anion exchange matrix, a Resource Q and a Superdex 200-pg size exclusion column.[38] All chromatographic materials were from Amersham Bioscience, Freiburg, Germany. Identity of the proteins was confirmed by matrix-assisted laser desorption ionisation (MALDI) mass spectrometry and Western blotting. The proteins were stored in 40 mM Hepes (pH 7.5), 150 mM KCl at −80 °C.

Reduction and oxidation of the Hsp26 cysteine variant

$Hsp26_{S4C}$ was reduced with a tenfold molar excess of $DTT_{(red)}$ or GSH in 40 mM Hepes (pH 7.5) for 120 minutes at room temperature, or overnight at 4 °C, respectively. Free reducing agents were removed using a 5 ml Desalting SEC (Amersham Bioscience, Freiburg, Germany). Re-oxidation of the cysteine residues was blocked by covalent modification with a 100-fold excess of IAA for 60 minutes at room temperature. Free IAA was removed as described for DTT. Oxidation of the protein was carried out with a tenfold molar excess of $DTT_{(ox)}$ or GSSG. The samples were purified using a 5 ml desalting SEC. The efficiency of reduction and oxidation was determined with DTNB.[46]

Circular dichroism spectroscopy for secondary and tertiary structure analysis

Far and near UV CD measurements were carried out in a Jasco J-715 spectropolarimeter (Jasco, Gross-Umstadt, Germany) equipped with a PTC343 peltier unit. The proteins were dialyzed against 10 mM potassium phosphate (pH 7.5) overnight at 4 °C. CD signals were accumulated ten times from 250 nm to 195 nm and 320 nm to 260 nm, respectively, using a scanning rate of 20 nm/minute. Far UV measurements were carried out at 20 °C. Near UV spectra were recorded at 25 °C and 45 °C, respectively. The molecular ellipticities were calculated for the mean residue weight (MRW) using the equation: $[\Theta]_{MRW} = \Theta \times 100 \times M_R / d \times c \times N_{aa}$, where Θ represents the measured ellipticities in degree, M_R the molecular

mass of the protein in g/mol, d the layer thickness in cm, c the sample concentration in mg/ml and N_{aa} the number of residues. Deconvolution of far UV spectra for secondary structure prediction was carried out using the CDNN software.[47]

Thermodynamic stability measurements

To monitor differences in thermal stability Hsp26, oxidized and reduced $Hsp26_{S4C}$ were equilibrated in 10 mM potassium phosphate (pH 7.5) overnight at 4 °C. The thermal unfolding and refolding was monitored in a Jasco J-715 spectropolarimeter equipped with a PTC343 peltier unit (Jasco, Gross-Umstadt, Germany). Signals of 0.1 mg/ml were recorded at $\lambda = 220$ nm. The samples were heated from 20 °C to 55 °C and cooled *vice versa* using a heating and cooling rate of 10 deg. C/hour. The thermal stabilities were calculated from reversible experiments assuming a simple two-state model for the high and low affinity states of Hsp26 as described by Pace & Scholtz.[48] We assumed a theoretical ΔC_p of 10,650 J mol^{-1} K^{-1}.[48]

Analytical size exclusion chromatography

A TosoHaas TSK G4000PW (30 cm × 0.75 cm) gel filtration column with a separating range from 10 to 1500 kDa was used (Tosoh Bioscience, Stuttgart, Germany). All experiments were performed at either 25 °C or 44 °C. Temperature was maintained using a temperature adjustable column oven (Jasco, Gross-Umstadt, Germany). All experiments were performed in 40 mM Hepes (pH 7.5), 150 mM KCl, 5 mM EDTA with 1 mM $DTT_{(red)}$ or 1 mM $DTT_{(ox)}$, respectively, using a flow rate of 0.5 ml/minute. Detection was with a Jasco FP 920 fluorescence detector, using an excitation wavelength of 275 nm and an emission wavelength of 307 nm.

Analytical ultracentrifugation

To determine the sedimentation coefficients of Hsp26 and Hsp26ΔN, analytical sedimentation ultracentrifugation was carried out using a Beckman XL-A ultracentrifuge equipped with a UV/VIS and interference detection unit (Beckman Coulter, Krefeld, Germany). The sample concentration was varied from 2 mg/ml to 0.1 mg/ml in 40 mM Hepes (pH 7.5). The samples were equilibrated at the corresponding temperature for four hours at 3000 rpm. Sedimentation was carried out in a TI-60 rotor, using a final rotation speed of 50,000 rpm. Detection was at 280 nm recording UV scans every six minutes. Evaluation of the data was carried out with the UltraScan software using the van Holde–Weischet velocity analysis.†

Thermal aggregation of CS

CS aggregation assays were carried out as described by Buchner *et al*.[49,50] In short, CS aggregates quantitatively at temperatures above 40 °C. The aggregation was followed at 340 nm recording the changes in absorbance signal in an Amersham Bioscience 4060 UV/VIS spectrophotometer equipped with a temperature-adjustable cuvette holder (Amersham Bioscience, Freiburg, Germany). To determine the chaperone activity increasing concentrations of Hsp26 were pre-incubated at 44 °C in 40 mM Hepes (pH 7.5). Substrate aggregation was induced by diluting the substrate to a final concentration of 1 μM into the pre-heated cuvette. The heat-induced aggregation of CS was normalized to 1.

Chemically induced aggregation of CS

CS was unfolded in 40 mM Hepes (pH 7.5), 6 M GdmCl following the protocol described by Buchner *et al*.[51] Aggregation of CS was induced by diluting the substrate 100-fold to a final concentration of 150 nM into 40 mM Hepes (pH 7.5) with 2 mM GSH or 1 mM GSSG, respectively. Aggregation was monitored at 25 °C in a SPEX Fluoromax-1 fluorescence spectrometer (Jobin Yvon, Munich, Germany) at an excitation and emission wavelength of $\lambda = 350$ nm. To monitor the temperature activation and inactivation of Hsp26, the proteins were incubated in the sample buffers at 50 °C for 20 minutes. The samples were then diluted tenfold into the cuvette and equilibrated for ten seconds at 25 °C. Subsequently, the aggregation of CS was induced as described above. The half-life of CS aggregation was derived from the half maximal light scatter signal.

Complex formation of Hsp26 and the cysteine variant with substrate proteins

To test if the reduced and oxidized form of $Hsp26_{S4C}$ differ in activity, 2 μM of each variant were co-incubated with 1 μM CS at 44 °C for 30 minutes in 40 mM Hepes (pH 7.5). Samples were then incubated on ice for ten minutes, centrifuged at 15,000*g* for one minute, and analyzed by analytical SEC and TEM.

Electron microscopy of Hsp26–substrate complexes

Complex formation of Hsp26 and the cysteine variants with CS was performed following the protocol used for the substrate complex formation experiments. The samples were directly applied to glow-discharged carbon-coated copper grids and negatively stained with 3% uranyl acetate. Electron micrographs were recorded at a nominal magnification of 33,000× using a Jeol 100CX electron microscope (Jeol, Eching, Germany) operating at 100 kV.

Subunit exchange measurements

Subunit exchange between Hsp26 complexes was monitored by fluorescence resonance energy transfer (FRET) in 40 mM Hepes (pH 7.5). $Hsp26_{S4C}$ was labelled with LYI or AIAS and Hsp26 with FITC or TAMRA. The labelling procedure was in accordance to the manufacturer's protocol (Molecular Probes, Karlsruhe, Germany). Subunit exchange was measured at a final concentration of 10 μM Hsp26 or 1 μM $Hsp26_{S4C}$, respectively, in 40 mM Hepes (pH 7.5) in a SPEX Fluoromax-1 fluorescence spectrophotometer (Jobin Yvon, Munich, Germany), monitoring the time-dependent changes in emission spectra or changes in the donor and acceptor signals, respectively. Excitation of AIAS labelled $Hsp26_{S4C}$ was at 336 nm and of FITC labelled Hsp26 at 495 nm. The reversibility of the process was controlled by the subsequent addition of a 40-fold excess of unlabelled protein to the mixed oligomers. The rate of subunits exchange was determined as described by Bova *et al*.[29] The half-life was calculated from $t_{1/2} = \ln 2/k_{transfer}$.

† http://www.ultrascan.uthscsa.edu

Acknowledgements

Hsp26ΔN was a kind gift from Thusnelda Stromer. We are indebted to Martin Heßling and Lin Müller for discussions. Bettina Richter is acknowledged for TEM assistance. We thank Helmut Krause and Anja Osterauer for support with mass spectrometry and protein purification. We also thank Birgit Meinlschmidt, Martin Haslbeck and Daniel Weinfurtner for reading the manuscript. This work was funded by the grants of the Deutsche Forschungsgesellschaft to J.B. and S.W.

References

1. Lindquist, S. & Craig, E. A. (1988). The heat-shock proteins. *Annu. Rev. Genet.* **22**, 631–677.
2. Walter, S. & Buchner, J. (2002). Molecular chaperones—cellular machines for protein folding. *Angew. Chem., Int. Ed Engl.* **41**, 1098–1113.
3. Jakob, U., Gaestel, M., Engel, K. & Buchner, J. (1993). Small heat shock proteins are molecular chaperones. *J. Biol. Chem.* **268**, 1517–1520.
4. Ehrnsperger, M., Graber, S., Gaestel, M. & Buchner, J. (1997). Binding of non-native protein to Hsp25 during heat shock creates a reservoir of folding intermediates for reactivation. *EMBO J.* **16**, 221–229.
5. Haslbeck, M. (2002). sHsps and their role in the chaperone network. *Cell Mol. Life Sci.* **59**, 1649–1657.
6. Stromer, T., Ehrnsperger, M., Gaestel, M. & Buchner, J. (2003). Analysis of the interaction of small heat shock proteins with unfolding proteins. *J. Biol. Chem* **278**, 18015–18021.
7. Haslbeck, M., Braun, N., Stromer, T., Richter, B., Model, N., Weinkauf, S. & Buchner, J. (2004). Hsp42 is the general small heat shock protein in the cytosol of *Saccharomyces cerevisiae*. *EMBO J.* **23**, 638–649.
8. Basha, E., Lee, G. J., Demeler, B. & Vierling, E. (2004). Chaperone activity of cytosolic small heat shock proteins from wheat. *Eur. J. Biochem.* **271**, 1426–1436.
9. De Jong, W. W., Caspers, G. J. & Leunissen, J. A. (1998). Genealogy of the alpha-crystallin–small heat-shock protein superfamily. *Int. J. Biol. Macromol.* **22**, 151–162.
10. Mornon, J. P., Halaby, D., Malfois, M., Durand, P., Callebaut, I. & Tardieu, A. (1998). alpha-Crystallin C-terminal domain: on the track of an Ig fold. *Int. J. Biol. Macromol.* **22**, 219–227.
11. Sun, T. X., Das, B. K. & Liang, J. J. (1997). Conformational and functional differences between recombinant human lens alphaA- and alphaB-crystallin 2. *J. Biol. Chem.* **272**, 6220–6225.
12. Narberhaus, F. (2002). Alpha-crystallin-type heat shock proteins: socializing minichaperones in the context of a multichaperone network. *Microbiol. Mol. Biol. Rev.* **66**, 64–93.
13. Horwitz, J. (1992). Alpha-crystallin can function as a molecular chaperone. *Proc. Natl Acad. Sci. USA*, **89**, 10449–10453.
14. Horwitz, J. (2003). Alpha-crystallin. *Expt. Eye Res.* **76**, 145–153.
15. Kim, K. K., Kim, R. & Kim, S. H. (1998). Crystal structure of a small heat-shock protein. *Nature*, **394**, 595–599.
16. van Montfort, R. L., Basha, E., Friedrich, K. L., Slingsby, C. & Vierling, E. (2001). Crystal structure and assembly of a eukaryotic small heat shock protein. *Nature Struct. Biol.* **8**, 1025–1030.
17. Leroux, M. R., Melki, R., Gordon, B., Batelier, G. & Candido, E. P. (1997). Structure–function studies on small heat shock protein oligomeric assembly and interaction with unfolded polypeptides. *J. Biol. Chem.* **272**, 24646–24656.
18. Haley, D. A., Bova, M. P., Huang, Q. L., Mchaourab, H. S. & Stewart, P. L. (2000). Small heat-shock protein structures reveal a continuum from symmetric to variable assemblies. *J. Mol. Biol.* **298**, 261–272.
19. Stromer, T., Fischer, E., Richter, K., Haslbeck, M. & Buchner, J. (2004). Analysis of the regulation of the molecular chaperone Hsp26 by temperature-induced dissociation: the N-terminal domail is important for oligomer assembly and the binding of unfolding proteins. *J. Biol. Chem.* **279**, 11222–11228.
20. Haslbeck, M., Ignatiou, A., Saibil, H., Helmich, S., Frenzl, E., Stromer, T. & Buchner, J. (2004). A domain in the N-terminal part of Hsp26 is essential for chaperone function and oligomerization. *J. Mol. Biol.* **343**, 445–455.
21. Giese, K. C. & Vierling, E. (2004). Mutants in a small heat shock protein that affect the oligomeric state. Analysis and allele-specific suppression. *J. Biol. Chem.* **279**, 32674–32683.
22. Carver, J. A., Esposito, G., Schwedersky, G. & Gaestel, M. (1995). ^{1}H NMR spectroscopy reveals that mouse Hsp25 has a flexible C-terminal extension of 18 amino acids. *FEBS Letters*, **369**, 305–310.
23. Fernando, P., Abdulle, R., Mohindra, A., Guillemette, J. G. & Heikkila, J. J. (2002). Mutation or deletion of the C-terminal tail affects the function and structure of *Xenopus laevis* small heat shock protein, hsp30. *Comput. Biochem. Physiol. B Biochem. Mol. Biol.* **133**, 95–103.
24. Lindner, R. A., Carver, J. A., Ehrnsperger, M., Buchner, J., Esposito, G., Behlke, J. *et al*. (2000). Mouse Hsp25, a small shock protein. The role of its C-terminal extension in oligomerization and chaperone action. *Eur. J. Biochem.* **267**, 1923–1932.
25. Raman, B. & Rao, C. M. (1997). Chaperone-like activity and temperature-induced structural changes of alpha-crystallin. *J. Biol. Chem.* **272**, 23559–23564.
26. Kokke, B. P., Leroux, M. R., Candido, E. P., Boelens, W. C. & De Jong, W. W. (1998). *Caenorhabditis elegans* small heat-shock proteins Hsp12.2 and Hsp12.3 form tetramers and have no chaperone-like activity. *FEBS Letters*, **433**, 228–232.
27. Guo, Z. & Cooper, L. F. (2000). An N-terminal 33-amino-acid-deletion variant of hsp25 retains oligomerization and functional properties. *Biochem. Biophys. Res. Commun.* **270**, 183–189.
28. Studer, S., Obrist, M., Lentze, N. & Narberhaus, F. (2002). A critical motif for oligomerization and chaperone activity of bacterial alpha-heat shock proteins. *Eur. J. Biochem.* **269**, 3578–3586.
29. Bova, M. P., Huang, Q., Ding, L. & Horwitz, J. (2002). Subunit exchange, conformational stability, and chaperone-like function of the small heat shock protein 16.5 from *Methanococcus jannaschii*. *J. Biol. Chem.* **277**, 38468–38475.
30. Bova, M. P., Ding, L. L., Horwitz, J. & Fung, B. K. (1997). Subunit exchange of alphaA-crystallin. *J. Biol. Chem.* **272**, 29511–29517.
31. Sobott, F., Benesch, J. L., Vierling, E. & Robinson, C. V. (2002). Subunit exchange of multimeric protein complexes. Real-time monitoring of subunit exchange

between small heat shock proteins by using electrospray mass spectrometry. *J. Biol. Chem.* **277**, 38921–38929.
32. Wintrode, P. L., Friedrich, K. L., Vierling, E., Smith, J. B. & Smith, D. L. (2003). Solution structure and dynamics of a heat shock protein assembly probed by hydrogen exchange and mass spectrometry. *Biochemistry*, **42**, 10667–10673.
33. Lentze, N., Aquilina, J. A., Lindbauer, M., Robinson, C. V. & Narberhaus, F. (2004). Temperature and concentration-controlled dynamics of rhizobial small heat shock proteins. *Eur. J. Biochem.* **271**, 2494–2503.
34. Susek, R. E. & Lindquist, S. L. (1989). hsp26 of *Saccharomyces cerevisiae* is related to the superfamily of small heat shock proteins but is without a demonstrable function. *Mol. Cell Biol.* **9**, 5265–5271.
35. Bossier, P., Fitch, I. T., Boucherie, H. & Tuite, M. F. (1989). Structure and expression of a yeast gene encoding the small heat-shock protein Hsp26. *Gene*, **78**, 323–330.
36. Tuite, M. F., Bentley, N. J., Bossier, P. & Fitch, I. T. (1990). The structure and function of small heat shock proteins: analysis of the *Saccharomyces cerevisiae* Hsp26 protein. *Antonie Van Leeuwenhoek*, **58**, 147–154.
37. Bentley, N. J., Fitch, I. T. & Tuite, M. F. (1992). The small heat-shock protein Hsp26 of *Saccharomyces cerevisiae* assembles into a high molecular weight aggregate. *Yeast*, **8**, 95–106.
38. Haslbeck, M., Walke, S., Stromer, T., Ehrnsperger, M., White, H. E., Chen, S. *et al*. (1999). Hsp26: a temperature-regulated chaperone. *EMBO J.* **18**, 6744–6751.
39. Murai, N., Makino, Y. & Yoshida, M. (1996). GroEL locked in a closed conformation by an interdomain cross-link can bind ATP and polypeptide but cannot process further reaction steps. *J. Biol. Chem.* **271**, 28229–28234.
40. Fasman, G. D. (1996). *Circular Dichroism and the Conformational Analysis of Biomolecules*, Plenum Press, New York.
41. Bova, M. P., Mchaourab, H. S., Han, Y. & Fung, B. K. (2000). Subunit exchange of small heat shock proteins. Analysis of oligomer formation of alphaA-crystallin and Hsp27 by fluorescence resonance energy transfer and site-directed truncations. *J. Biol. Chem.* **275**, 1035–1042.
42. Haley, D. A., Horwitz, J. & Stewart, P. L. (1999). Image restrained modeling of alphaB-crystallin. *Expt. Eye Res.* **68**, 133–136.
43. van Montfort, R. L., Basha, E., Friedrich, K. L., Slingsby, C. & Vierling, E. (2001). Crystal structure and assembly of a eukaryotic small heat shock protein. *Nature Struct. Biol.* **8**, 1025–1030.
44. Raman, B., Ramakrishna, T. & Rao, C. M. (1995). Temperature dependent chaperone-like activity of alpha-crystallin. *FEBS Letters*, **365**, 133–136.
45. Raman, B. & Rao, C. M. (1994). Chaperone-like activity and quaternary structure of alpha-crystallin. *J. Biol. Chem.* **269**, 27264–27268.
46. Evans, J. C. & Ellman, G. L. (1959). The ionization of cysteine. *Biochim. Biophys. Acta*, **33**, 574–576.
47. Bohm, G., Muhr, R. & Jaenicke, R. (1992). Quantitative analysis of protein far UV circular dichroism spectra by neural networks. *Protein Eng.* **5**, 191–195.
48. Myers, J. K., Pace, C. N. & Scholtz, J. M. (1995). Denaturant m values and heat capacity changes: relation to changes in accessible surface areas of protein unfolding. *Protein Sci.* **4**, 2138–2148.
49. Kiefhaber, T., Rudolph, R., Kohler, H. H. & Buchner, J. (1991). Protein aggregation *in vitro* and *in vivo*: a quantitative model of the kinetic competition between folding and aggregation. *Nature Biotechnol.* **9**, 825–829.
50. Buchner, J., Grallert, H. & Jakob, U. (1998). Analysis of chaperone function using citrate synthase as non-native substrate protein. *Methods Enzymol.* **290**, 323–338.
51. Buchner, J., Schmidt, M., Fuchs, M., Jaenicke, R., Rudolph, R., Schmid, F. X. & Kiefhaber, T. (1991). GroE facilitates refolding of citrate synthase by suppressing aggregation. *Biochemistry*, **30**, 1586–1591.

Edited by K. Kuwajima

(Received 16 March 2005; received in revised form 28 April 2005; accepted 18 May 2005)